

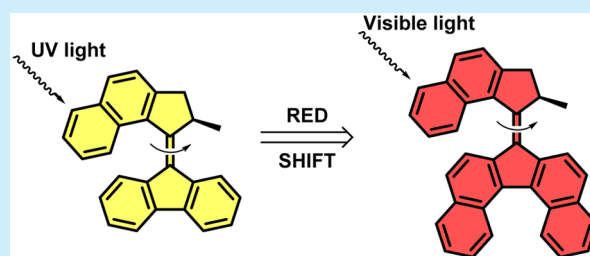
Visible-Light Excitation of a Molecular Motor with an Extended Aromatic Core

Thomas van Leeuwen, Jasper Pol, Diederik Roke, Sander J. Wezenberg,¹ and Ben L. Feringa^{1*}

Stratingh Institute for Chemistry, University of Groningen, Nijenborgh 4, 9747 AG Groningen, The Netherlands

S Supporting Information

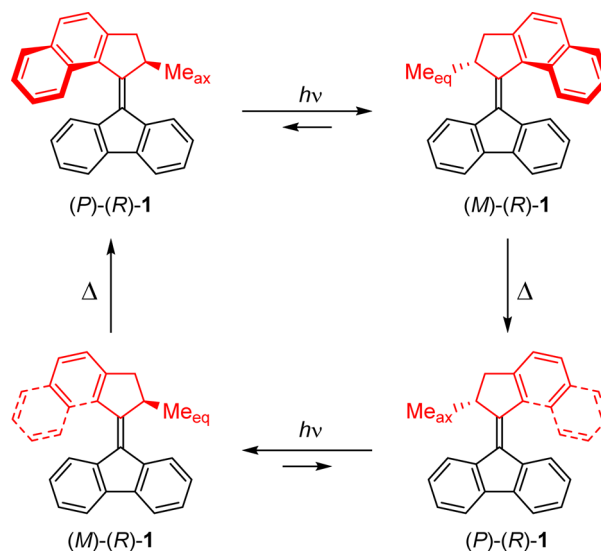
ABSTRACT: Exploring routes to visible-light-driven rotary motors, the possibility of red-shifting the excitation wavelength of molecular motors by extension of the aromatic core is studied. Introducing a dibenzofluorenyl moiety in a standard molecular motor resulted in red-shifting of the absorption spectrum. UV/vis and ¹H NMR spectroscopy showed that these motors could be isomerized with light of wavelengths up to 490 nm and that the structural modification did not impair the anticipated rotary behavior. Extension of the aromatic core is therefore a suitable strategy to apply in pursuit of visible-light-driven molecular motors.



Molecular switches and motors are increasingly applied in molecular machines¹ and to control the properties of materials² as well as biological systems.³ The incorporation of light-addressable switches into chemical and biological systems allows for the tuning of property and function with high spatiotemporal resolution. A potential drawback is the use of UV light to achieve switching, as it can cause damage to the material. Red-shifting the excitation wavelength of photoswitches and motors in order to reduce undesired side effects and to increase their applicability in, e.g., soft materials or biological systems, continues to be one of the major challenges.⁴ Various strategies have been reported to red-shift the excitation wavelength of well-established photoswitches such as azobenzenes and diarylethenes. The ortho-functionalization of azobenzenes with, e.g., methoxy, fluorine, chlorine, or thioether groups,⁵ the introduction of an electron donor–acceptor pair,⁶ or the extension of the aromatic core has been successful in achieving the visible-light excitation of azobenzenes. Bridging of azobenzenes also afforded photoswitches operable in the far red region.⁷ For diarylethenes, the extension of the π system⁸ or the covalent linkage of triplet sensitizers afforded switches with red-shifted absorption spectra.⁹ New photoswitches which can be operated with visible light are also being developed.¹⁰

Light-driven molecular motors based on overcrowded alkenes are unique among photoswitches, since their photoexcitation leads to unidirectional rotation around their central axis (Scheme 1).¹¹ Irradiation of a typical motor **1** with the stereogenic methyl group in the pseudoaxial position leads to the formation of a metastable isomer having the methyl group in a pseudoequatorial position. This metastable isomer can relax to the more stable isomer via a thermal helix inversion (THI) in which the upper half flips over the lower half. A second irradiation and thermal step leads to the 360° unidirectional rotation around the double bond. If the temperature is kept below a certain threshold, the THI slows

Scheme 1. Unidirectional Rotation of Motor 1



down, and these molecules can function as multistate switches. Both its repetitive unidirectional rotation upon continuous irradiation as well as its multistate switching have been used to achieve dynamic control of its function.¹²

Several successful approaches have been reported on how to rotate molecular motors with visible light. In 2003, we showed that the introduction of a push–pull system in the lower half allows these systems to be operated with 430 nm light.¹³ The use of photosensitizers employing either a palladium porphyrin¹⁴ or a ruthenium complex¹⁵ also proved to be an effective approach in achieving visible-light excitation. Fur-

Received: January 30, 2017

Published: March 1, 2017

thermore, Dube and co-workers developed a hemithioindigo motor which can be driven by light up to 500 nm.¹⁶

Here, we explore for the first time the possibility of red-shifting the excitation wavelength by extension of the aromatic core of the molecular motor. This strategy has not been successfully applied yet but could be pivotal toward the application of molecular motors in biological systems or artificial molecular machines. Nevertheless, to move the excitation wavelength into the visible region is challenging since modification of the structural and electronic properties might perturb the motor functioning. Increasing the steric bulk around the fjord region could hamper the thermal helix inversion, and therefore, we opted to extend the lower part of the common well-studied motor **1** to obtain motor **2** (Figure 1). TD-DFT (B3LYP 6-31G(d,p)) was employed to predict

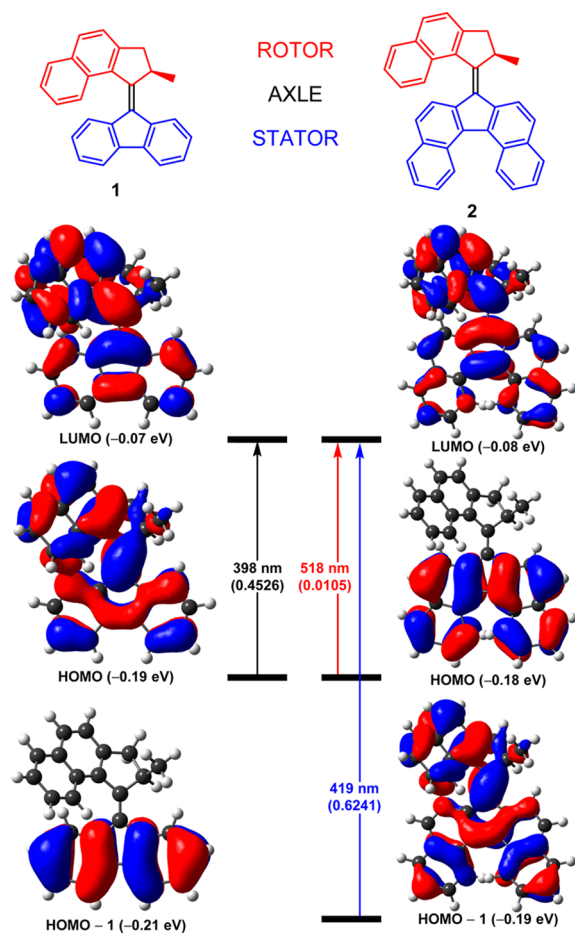


Figure 1. Structures and selected molecular orbitals of **1** (left) and **2** (right). Oscillator strength of selected transitions are given in parentheses (see the SI).

how this structural modification affects the absorption properties of **2** (Figure 1). It was found for the known motor **1** that the absorption maximum can be accurately predicted by this method (experimental: 395 nm¹⁷ vs predicted: 398 nm). For motor **2**, it is anticipated that the HOMO–LUMO gap is significantly reduced. The first calculated transition of 518 nm has, however, a low oscillator strength (0.0105), and considering the molecular orbitals involved in this transition, it is doubtful whether the excitation of this transition would lead to the isomerization of the double bond. The second lowest energy transition (HOMO–1 → LUMO: 419 nm)

resembles more closely (in terms of molecular orbitals) the HOMO–LUMO transition of **1**, for which excitation does lead to photoisomerization of the central double bond.¹⁷ These results indicate that extension of the aromatic core in the lower half would result in a red-shift of the wavelength at which these molecules can undergo photoisomerization.

DFT at the B3LYP/6-31G(d,p) level was also employed in order to investigate how the structural modification affects the thermal isomerization reaction of **2**. First, the ground states and transition states (TS) were located using potential energy scans, followed by a geometry optimization and frequency analysis.

It was found that the dibenzofluorenyl lower half of **2** adopts a helical conformation, reminiscent of the structure of helicenes. Motor **2**, therefore, has three stereochemical elements, i.e., the helicity in the upper and lower halves and the stereogenic carbon center. Hence, for (*R*)-**2**, four diastereoisomers exist. The optimized structures of the ground states, the TSs, and their corresponding Gibbs free energies were calculated (Figure 2 and Figure S10). It is remarkable that for the photogenerated metastable state the *P* helical conformation in the lower half is preferred, while for the stable form the *M* helicity is thermodynamically favored. Comparison of the barrier for THI for **2** ($\Delta^\ddagger G_{\text{calc}} = 95.5 \text{ kJ/mol}^{18}$) with the experimentally obtained barrier for THI of **1** ($\Delta^\ddagger G_{\text{exp}} = 86 \text{ kJ/mol}$,¹⁷ $\Delta^\ddagger G_{\text{calcd}} = 88.5 \text{ kJ/mol}$) leads to the expectation that the rotational speed decreases slightly upon this extension of the aromatic core. The synthesis and study of **2** were therefore pursued to confirm this hypothesis.

In line with the reported syntheses of structurally related overcrowded alkenes, it was opted to construct the sterically hindered double bond employing a Barton–Kelllogg reaction (Scheme 2). Diazo **3** was prepared by the conversion of the known ketone **4**¹⁹ into its corresponding hydrazone **5** with hydrazine, followed by an oxidation using MnO₂. The preparation of thioketone **6** has been reported before,²⁰ and it was coupled to **3** at room temperature to afford the final product **2** in 18% yield (two steps from **5**).

UV/vis spectroscopy was used to follow the photochemical isomerization of **2** (Figure 3). The irradiation of **2** in CH₂Cl₂ at 20 °C gave rise to a bathochromic shift in the UV/vis spectrum with clear isosbestic points, indicative of the formation of the metastable form. It was confirmed by using different wavelengths of light that **2** undergoes photochemical isomerization with wavelengths up to 490 nm. The photostationary state (PSS) ratio at $\lambda_{\text{max}} = 490 \text{ nm}$ based on the spectral changes in the UV/vis absorption was quite low, since the photogenerated metastable state absorbs strongly in that region. The highest PSS ratio (76:24 (metastable/stable)) was obtained when 420 nm irradiation was employed.

The photochemical isomerization of **2** at 420 nm was also followed by ¹H NMR spectroscopy. A solution of **2** in CD₂Cl₂ was cooled to –40 °C and irradiated at 420 nm (Figure S5).

The characteristic shift in the ¹H NMR spectrum of the stereogenic methyl group (*H*_a: 1.42 ppm → 1.71 ppm) confirm that the moiety adopts a pseudoequatorial position upon isomerization of the double bond. Other notable shifts include the shift in the methylene hydrogens (*H*_b: 2.89 ppm → 3.29 ppm) and (*H*_b′: 3.65 ppm → 3.70 ppm) and the stereogenic hydrogen (*H*_c: 4.51 ppm → 4.41 ppm), which can all be assigned to the formation of the metastable state and is in accordance with related motor **1**. A PSS ratio of 76:24 (metastable/stable) was found by integration of the NMR peaks.²¹

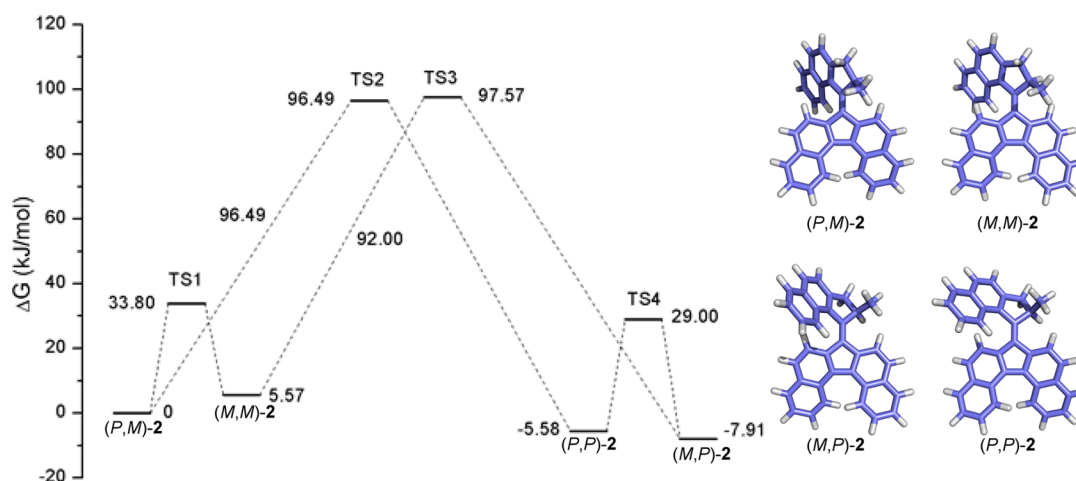


Figure 2. Energy diagram of the interconversion of the diastereoisomers of **2**. Nomenclature is defined as follows: For (P,M) -**2**, the first stereochemical descriptor (P) denotes the helicity in the lower half, while the second descriptor (M) denotes the helicity in the upper half. The optimized structures of the transition states are depicted in Figure S10.

Scheme 2. Synthesis of Molecular Motor **2**

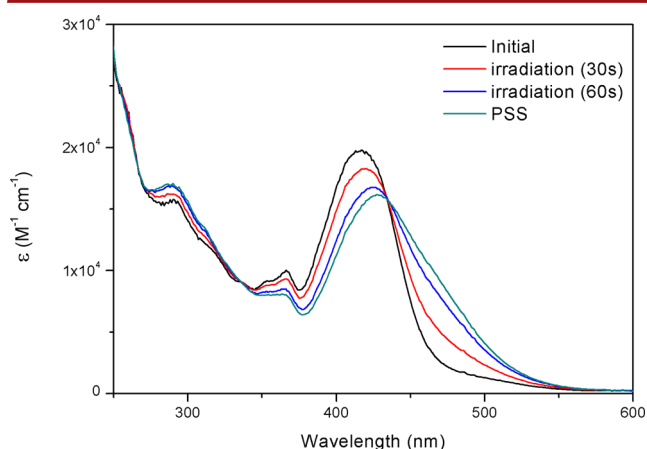
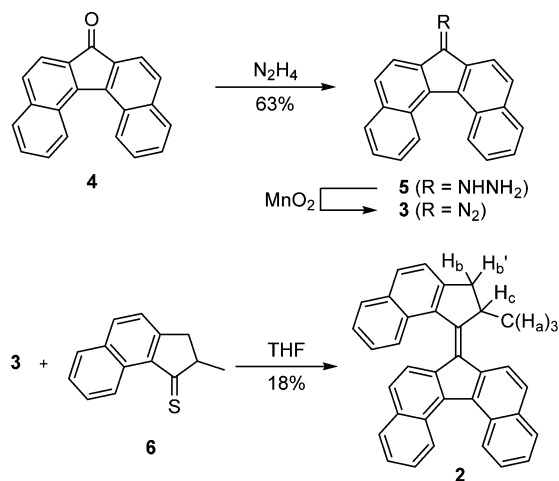


Figure 3. Changes in the UV/vis absorption spectrum of a solution of **2** in CH_2Cl_2 upon irradiation with $\lambda_{\text{max}} = 420 \text{ nm}$.

From the results obtained by UV/vis and ^1H NMR spectroscopy, it can be concluded that **2** exhibits the anticipated isomerization behavior. After it was established that the photochemistry still works accordingly, the subsequent thermal relaxation was studied. The kinetics of the process was followed

at six temperatures between 10 and 35 °C. The Gibbs free energy of activation of the thermal helix inversion was determined using the Eyring equation and was $93.9 \pm 1 \text{ kJ/mol}$ (Figure S10). The experimentally determined value is in agreement with the predicted Gibbs free energy of activation of 95.5 kJ/mol. Comparison of the $\Delta^\ddagger G^\circ$ of the THI for motor **2** ($\Delta^\ddagger G^\circ = 93.9 \pm 1 \text{ kJ/mol}$) and motor **1** ($\Delta^\ddagger G^\circ = 86 \text{ kJ/mol}$) reveals that the speed of rotation of motor **2** is slightly lower due to the structural modification, as anticipated on the basis of DFT calculations.

In conclusion, it was demonstrated that extension of the aromatic core of molecular motors is a viable strategy for red-shifting their excitation wavelength. To this end, a novel molecular motor with a dibenzofluorene lower half was designed and synthesized. It was found that the extension of the aromatic core allows for photoisomerization with visible light with wavelengths up to 490 nm, without impairing the motor function. Extension of the stator moiety is therefore a promising strategy that can be applied to other molecular motors as well. It will form a viable addition to the already existing methods for red-shifting the excitation wavelength of light-driven molecular motors. Further research focuses on employing electron-donating/acceptor groups in combination with extending the aromatic π system in order to reach even higher excitation wavelengths.

■ ASSOCIATED CONTENT

Supporting Information

The Supporting Information is available free of charge on the ACS Publications website at DOI: [10.1021/acs.orglett.7b00317](https://doi.org/10.1021/acs.orglett.7b00317).

Experimental procedures and analytical data of all title compounds (^1H NMR, ^{13}C NMR, and HRMS spectra), Eyring plot analysis, and computational results (PDF)

■ AUTHOR INFORMATION

Corresponding Author

*E-mail: b.l.feringa@rug.nl.

ORCID

Sander J. Wezenberg: [0000-0001-9192-3393](https://orcid.org/0000-0001-9192-3393)

Ben L. Feringa: 0000-0003-0588-8435

Notes

The authors declare no competing financial interest.

ACKNOWLEDGMENTS

Financial support from the Ministry of Education, Culture and Science (Gravity program 024.001.035), The Netherlands Organization for Scientific Research (NWO-CW, Veni Grant No. 722.014.006 to S.J.W.), European Research Council (Advanced Investigator Grant No. 694345 to B.L.F.), and NRSC catalysis are gratefully acknowledged. We thank J. C. M. Kistemaker for valuable discussions.

REFERENCES

- (1) (a) *Molecular Switches*; Browne, W. R.; Feringa, B. L., Eds.; Wiley-VCH: Weinheim, 2011. (b) *From Non-Covalent Assemblies to Molecular Machines*; Sauvage, J. P.; Gaspard, P., Eds.; Wiley-VCH: Weinheim, 2010. (c) *Molecular Devices and Machines: Concepts and Perspectives for the Nanoworld*; Balzani, V.; Credi, A.; Venturi, M., Eds.; Wiley-VCH: Weinheim, 2008. (d) Cheng, C.; Stoddart, J. F. *ChemPhysChem* **2016**, *17*, 1780. (e) Erbas-Cakmak, S.; Leigh, D. A.; McTernan, C. T.; Nussbaumer, A. L. *Chem. Rev.* **2015**, *115*, 10081. (f) Coskun, A.; Banaszak, M.; Astumian, R. D.; Stoddart, J. F.; Grzybowski, B. A. *Chem. Soc. Rev.* **2012**, *41*, 19. (g) Kinbara, K.; Aida, T. *Chem. Rev.* **2005**, *105*, 1377.
- (2) (a) Kundu, P. K.; Klajn, R. *ACS Nano* **2014**, *8*, 11913. (b) Spruell, J. M.; Hawker, C. J. *Chem. Sci.* **2011**, *2*, 18. (c) Qu, D. H.; Wang, Q. C.; Zhang, Q. W.; Ma, X.; Tian, H. *Chem. Rev.* **2015**, *115*, 7543. (d) Klajn, R. *Chem. Soc. Rev.* **2014**, *43*, 148. (e) Zhang, J.; Zou, Q.; Tian, H. *Adv. Mater.* **2013**, *25*, 378. (f) Russev, M. M.; Hecht, S. *Adv. Mater.* **2010**, *22*, 3348.
- (3) (a) Broichhagen, J.; Frank, J. A.; Trauner, D. *Acc. Chem. Res.* **2015**, *48*, 1947. (b) Dong, M.; Babalhavaeji, A.; Samanta, S.; Beharry, A. A.; Woolley, G. A. *Acc. Chem. Res.* **2015**, *48*, 2662. (c) Lerch, M. M.; Hansen, M. J.; van Dam, G. M.; Szymanski, W.; Feringa, B. L. *Angew. Chem., Int. Ed.* **2016**, *55*, 10978. (d) Velema, W. A.; Szymanski, W.; Feringa, B. L. *J. Am. Chem. Soc.* **2014**, *136*, 2178.
- (4) Bléger, D.; Hecht, S. *Angew. Chem., Int. Ed.* **2015**, *54*, 11338.
- (5) (a) Beharry, A. A.; Sadowski, O.; Woolley, G. A. *J. Am. Chem. Soc.* **2011**, *133*, 19684. (b) Bléger, D.; Schwarz, J.; Brouwer, A. M.; Hecht, S. *J. Am. Chem. Soc.* **2012**, *134*, 20597. (c) Konrad, D. B.; Frank, J. A.; Trauner, D. *Chem. - Eur. J.* **2016**, *22*, 4364. (d) Samanta, S.; McCormick, T. M.; Schmidt, S. K.; Seferos, D. S.; Woolley, G. A. *Chem. Commun.* **2013**, *49*, 10314. (e) Hansen, M. J.; Lerch, M. M.; Szymanski, W.; Feringa, B. L. *Angew. Chem., Int. Ed.* **2016**, *55*, 13514.
- (6) Goulet-Hanssens, A.; Corkery, T. C.; Priimagi, A.; Barrett, C. J. *J. Mater. Chem. C* **2014**, *2*, 7505.
- (7) (a) Siewertsen, R.; Neumann, H.; Buchheim-Stehn, B.; Herges, R.; Näther, C.; Renth, F.; Temps, F. *J. Am. Chem. Soc.* **2009**, *131*, 15594. (b) Hammerich, M.; Schütt, C.; Stähler, C.; Lenters, P.; Röhricht, F.; Höppner, R.; Herges, R. *J. Am. Chem. Soc.* **2016**, *138*, 13111.
- (8) Fukaminato, T.; Hirose, T.; Doi, T.; Hazama, M.; Matsuda, K.; Irie, M. *J. Am. Chem. Soc.* **2014**, *136*, 17145.
- (9) Fredrich, S.; Göstl, R.; Herder, M.; Grubert, L.; Hecht, S. *Angew. Chem., Int. Ed.* **2016**, *55*, 1208.
- (10) (a) Helmy, S.; Leibfarth, F. A.; Oh, S.; Poelma, J. E.; Hawker, C. J.; Read de Alaniz, J. R. *J. Am. Chem. Soc.* **2014**, *136*, 8169. (b) Hemmer, J. R.; Poelma, S. O.; Treat, N.; Page, Z. A.; Dolinski, N.; Diaz, Y. J.; Tomlinson, W.; Clark, K. D.; Hooper, J. P.; Hawker, C. J.; Read de Alaniz, J. R. *J. Am. Chem. Soc.* **2016**, *138*, 13960. (c) Lerch, M. M.; Wezenberg, S. J.; Szymanski, W.; Feringa, B. L. *J. Am. Chem. Soc.* **2016**, *138*, 6344.
- (11) (a) Koumura, N.; Zijlstra, R. W.; van Delden, R. A.; Harada, N.; Feringa, B. L. *Nature* **1999**, *401*, 152. (b) Koumura, N.; Geertsema, E. M.; Meetsma, A.; Feringa, B. L. *J. Am. Chem. Soc.* **2000**, *122*, 12005. (c) Feringa, B. L. *J. Org. Chem.* **2007**, *72*, 6635.
- (12) Selected examples: (a) Kudernac, T.; Ruangsupapichat, N.; Parschau, M.; Maciá, B.; Katsonis, N.; Harutyunyan, S. R.; Ernst, K.-H.; Feringa, B. L. *Nature* **2011**, *479*, 208. (b) Wang, J.; Feringa, B. L. *Science* **2011**, *331*, 1429. (c) Li, Q.; Fuks, G.; Moulin, E.; Maaloum, M.; Rawiso, M.; Kulic, I.; Foy, J. T.; Giuseppone, N. *Nat. Nanotechnol.* **2015**, *10*, 161. (d) Vlatkovic, M.; Feringa, B. L.; Wezenberg, S. J. *Angew. Chem., Int. Ed.* **2016**, *55*, 1001.
- (13) van Delden, R. A.; Koumura, N.; Schoevaars, A.; Meetsma, A.; Feringa, B. L. *Org. Biomol. Chem.* **2003**, *1*, 33.
- (14) Cnossen, A.; Hou, L.; Pollard, M. M.; Wesenhagen, P. V.; Browne, W. R.; Feringa, B. L. *J. Am. Chem. Soc.* **2012**, *134*, 17613.
- (15) Wezenberg, S. J.; Chen, K. Y.; Feringa, B. L. *Angew. Chem., Int. Ed.* **2015**, *54*, 11457.
- (16) Guentner, M.; Schildhauer, M.; Thumser, S.; Mayer, P.; Stephenson, D.; Mayer, P. J.; Dube, H. *Nat. Commun.* **2015**, *6*, 8406.
- (17) Pollard, M. M.; Wesenhagen, P. V.; Pijper, D.; Feringa, B. L. *Org. Biomol. Chem.* **2008**, *6*, 1605.
- (18) Since both metastable isomers are interconverting rapidly, they can relax via two pathways (via TS2 and TS3). This results in an overall reaction rate corresponding to a $\Delta^\ddagger G = 95.5$ kJ/mol.
- (19) Tian, Y.; Uchida, K.; Kurata, H.; Hirao, Y.; Nishiuchi, T.; Kubo, T. *J. Am. Chem. Soc.* **2014**, *136*, 12784.
- (20) Pijper, D.; Feringa, B. L. *Angew. Chem., Int. Ed.* **2007**, *46*, 3693.
- (21) This PSS ratio is comparable to that previously measured for **1** (PSS₃₆₅ = 75:25, see ref 17). Nevertheless, comparison of the initial rates of formation of the metastable state of **1** and **2** revealed that the photoconversion efficiency of both the forward and backward isomerization processes is lower for **2** than for **1** (Figure S6).